ELSEVIER

Journal of Hazardous Materials B101 (2003) 259–272

Journal of Hazardous Materials

www.elsevier.com/locate/jhazmat

Control of acid gases using a fluidized bed adsorber

Bo-Chin Chiang, Ming-Yen Wey*, Chia-Lin Yeh

Department of Environmental Engineering, Chung-Hsing University, Taichung 402, Taiwan, ROC

Received 4 October 2002; received in revised form 26 March 2003; accepted 14 April 2003

Abstract

During incineration, secondary pollutants such as acid gases, organic compounds, heavy metals and particulates are generated. Among these pollutants, the acid gases, including sulfur oxides (SO_x) and hydrogen chloride (HCl), can cause corrosion of the incinerator piping and can generate acid rain after being emitted to the atmosphere. To address this problem, the present study used a novel combination of air pollution control devices (APCDs), composed of a fluidized bed adsorber integrated with a fabric filter. The major objective of the work is to demonstrate the performance of a fluidized bed adsorber for removal of acid gases from flue gas of an incinerator. The adsorbents added in the fluidized bed adsorber were mainly granular activated carbon (AC; with or without chemical treatment) and with calcium oxide used as an additive. The advantages of a fluidized bed reactor for high mass transfer and high gas–solid contact can enhance the removal of acid gases when using a dry method.

On the other hand, because the fluidized bed can filter particles, fine particles prior to and after passing through the fluidized bed adsorber were investigated. The competing adsorption on activated carbon between different characteristics of pollutants was also given preliminary discussion. The results indicate that the removal efficiencies of the investigated acid gases, SO_2 and HCl, are higher than 94 and 87%, respectively. Thus, a fluidized bed adsorber integrated with a fabric filter has the potential to replace conventional APCDs, even when there are other pollutants at the same time.

Keywords: Incineration; Fluidized bed adsorber; Fabric filter; Activated carbon; Acid gases; Heavy metals; PAHs

1. Introduction

The incineration of solid waste produces large amounts of air pollutants and solid wastes, including sulfur oxides (SO_x), hydrogen chloride (HCl), carbon monoxide (CO), volatile

* Corresponding author. Tel.: +886-4-228-52455; fax: +886-4-228-62587.
E-mail address: mywey@dragon.nchu.edu.tw (M.-Y. Wey).

0304-3894/$ – see front matter © 2003 Elsevier B.V. All rights reserved.
doi:10.1016/S0304-3894(03)00141-9

organic compounds (VOCs), particulates, and heavy metals. Among these pollutants, acid gases such as SO_x have been studied worldwide since they are the major cause of acid rain and fog, which harm the natural environment and human life. The conventional technologies of desulfurization are wet, dry and semi-dry mechanisms using limestone or lime. Wet desulfurization requires a large amount of space and high capital costs, especially for the wastewater purification [1]. Lower desulfurization efficiency is the main disadvantage of the dry method, although it has lower capital cost. Spray–dryer systems have been widely employed recently due to their high desulfurization efficiency, but they are more limited based on stoichiometry.

In recent years, there has been research on sulfur dioxide (SO_2) removal over carbon or carbon-based materials. In order to enhance removal efficiency and decrease the cost, the pretreatment of carbon or carbon-based materials, including chemical and physical treatment have been widely studied [1–6]. The physical treatments include feeding nitrogen (N_2), oxygen (O_2), helium (He), carbon dioxide (CO_2), air and steam at high temperatures (200–1000 °C), which can oxidize and activate the carbon or carbon-based materials by increasing the surface area, oxygen content, and micropores; as well as decreasing volatile compounds and carbon–oxygen (C–O) complexes. In addition chemical treatments such as immersion in nitric acid (HNO_3), hydrogen peroxide (H_2O_2), or potassium hydroxide (KOH) can increase the surface area, oxygen deposition and acidity and decrease basicity. Some researchers have investigated the effect of specific surface area, pore size distribution, acidic and basic surface chemical groups, as well as metallic derivatives on the adsorption of SO_2 over carbon or carbon-based materials [2,3,6–9]. The results indicate that the surface area is not a directly proportion factor for SO_2 removal over carbon, but rather a pore size distribution less than 30–50 Å was the main requirement to remove SO_2. The nature of the surface acidic group was sufficiently known, although there were some doubts regarding the real nature of the basic surface sites.

As indicated above, adsorption mechanisms which capture SO_2 by carbon or carbon-based materials have been widely studied, but most of them are performed in fixed bed reactors using simulated feed streams with only a single pollutant present. However, there has been little study of adsorption processes in actual complex flue gas from an incinerator. In a previous study [10], a fluidized bed adsorber serving as an air pollution control device (APCD) was employed to control organics, with high removal efficiency. Similarly, the advantage of high mass transfer in a fluidized bed adsorber was also expected to improve the disadvantage (low desulfurization efficiency) of dry desulfurization in the present study. On the other hand, the fluidized reactor has the important characteristic of also removing particulates at the same time [11]. Although it has been shown that particle sizes larger than 34.1 μm can be filtered via a fluidized reactor [10], the ability of fluidized reactors to filter fine particles has not been determined. Therefore, in this study two sets of cascade impactors were used to sample fine particles prior to and after passing through the fluidized bed adsorber, and then the mass size distribution and elemental size distribution of fine particles were determined. In addition, a fabric filter integrated after the adsorber was used to further remove the remaining pollutants. Furthermore, the removal efficiency of other pollutants such as HCl, organics and heavy metals are also discussed, and the competition adsorption between pollutants is given preliminarily investigation.

Table 1
Elemental compositions of each simulated feed waste

Simulated feed wastes	Elements					
	C (%)	H (%)	O (%)	N (%)	Cl (%)	S (%)
LDPE[a]	85.26	14.82	–	–	–	–
PE[b] bag	85.70	14.30	–	–	–	–
PVC[c]	38.40	4.80	–	–	56.80	
S	–	–	–	–	–	99.90
Sawdust	44.20	5.15	38.35	12.30	–	–

[a] LDPE: low-density polyethylene.
[b] PE: polyethylene.
[c] PVC: polyvinyl chloride.

2. Experimental

2.1. Preparation of simulated feed wastes

In order to generate simulated flue gas streams containing acid gases, heavy metals and organic compounds, the following compounds were used as feedstock: sawdust, low-density polyethylene (LDPE) granules, polyvinyl chloride (PVC), sulfur powder, and a heavy metal solution (single or mixed). All the synthetic materials were enclosed in small polyethylene (PE) bags. The investigated metals lead (Pb), chromium (Cr) and cadmium (Cd) were dissolved in distilled water in nitrate form ($Pb(NO_3)_2$, $Cr(NO_3)_3$, and $Cd(NO_3)_2$). The elemental analyses of sawdust, LDPE granules, PVC and PE bag were performed before preparing the feedstock (Table 1). Table 2 lists the detailed compositions of the simulated feed wastes and operating conditions.

2.2. Preparation and pretreatment of adsorbent

The adsorbent used here contained granular activated carbon (AC), activated carbon pretreated with potassium hydroxide solution (AC + KOH) (immersed in five times weight of AC 4% KOH for 24 h and then cleaned with deionized water and dried in a 120 °C oven for 12 h) and lime (CaO). The commercial activated carbon (G-840) was made from coconut shells, as obtained from China Activated Carbon Industries Ltd., Taiwan, ROC. It was cleaned with deionized water, conditioned at 105 °C for 48 h, and then stored in a brown container.

The other adsorbent, lime (CaO), in lumpy form was obtained from commercially available chemical raw materials. To avoid being deliquesced, they were stored in desiccators after crushing and sieving to the investigated size. The weight of activated carbon used for each test was 270 g and CaO was 27 g (10%), 81 g (30%) or 135 g (50%). Table 3 lists the characteristics of adsorbents used in the present study. The physical characteristics such as Brunauer–Emmett–Teller (BET) specific surface area, total pore volume and average pore diameter were measured with a micromeritics surface area analyzer (ASAP 2010) that utilized the BET low-temperature N_2 adsorption technique.

Table 2
Composition of feedstock and operating conditions

Run	Feedstock (g per bag)		Adsorbent	Adsorption temperature (°C)
	Metal	Others		
1	Mixed (Pb, Cr, Cd: each for 0.029)		AC[a]	230
2	Mixed		AC + KOH	230
3	Mixed		AC + 10 wt.% CaO	230
4	Mixed	Sawdust: 1	AC + 30 wt.% CaO	230
5	Mixed	LDPE[b]: 0.4	AC + 50 wt.% CaO	230
6	0.029 Pb	PE[c] bag: 0.3	AC + 10 wt.% CaO	230
7	0.029 Cr	PVC[d]: 0.2	AC + 10 wt.% CaO	230
8	0.029 Cd	S: 0.033	AC + 10 wt.% CaO	230
9	Mixed		AC + 10 wt.% CaO	230
10	–		AC + 10 wt.% CaO	230
11	Mixed		AC + 10 wt.% CaO	180
12	Mixed		AC + 10 wt.% CaO	280

Note 1: The operating gas velocity of fluidized bed adsorber was $U_f/U_{mf} = 2$. U_f: fluidized velocity; U_{mf}: minimum gas velocity for fluidization. *Note* 2: Impactor sampling were performed in Runs 6–10.

[a] AC: activated carbon.

[b] LDPE: low-density polyethylene.

[c] PE: polyethylene.

[d] PVC: polyvinyl chloride.

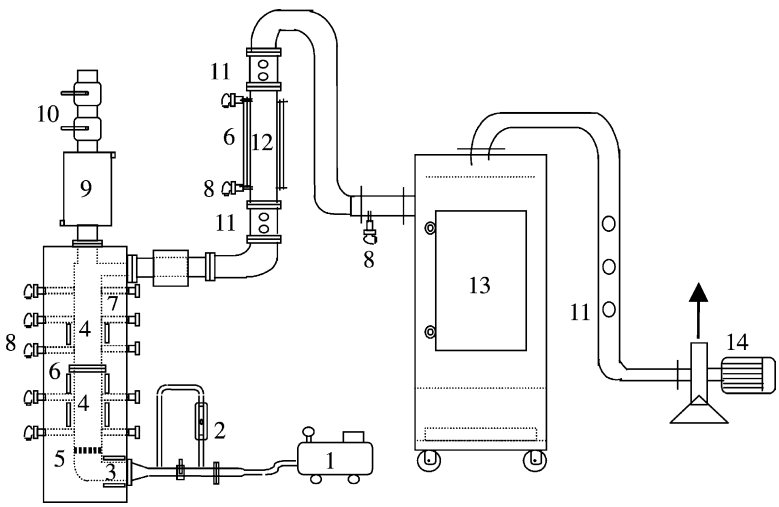

Fig. 1. Fluidized bed incinerator: (1) blower, (2) flow meter, (3) preheated chamber, (4) major combustion chamber, (5) air distribution, (6) electrical heater, (7) thermal insulator, (8) thermocouples, (9) cold chamber, (10) feeder, (11) sampling location, (12) fluidized bed adsorber, (13) fabric filter, (14) induced fan.

Table 3
Characteristics of adsorbents

Adsorbent	Characteristic	Value
Activated carbon (AC[a]) (G-840)	Particle size[b] (μm)	710–840
	Total surface area (BET[c], N_2)[b] (m^2/g)	1075
	Average pore diameter[b] (Å)	19.7
	Ball-pan hardness (%)	≥98
	Moisture as packed (%)	≤5
	Ash (%)	≤3
	Iodine number (mg/g)	≥1050
	Bulk density (g/cm^3)	0.48–0.52
	Toluene adsorption (%)	≥33
	Activity-CCl_4 (%)	≥98
	pH of water extract	6.0–8.0
	Methylene blue number (ml)	≥200
	Abrasion number	≥96
Activated carbon pretreated with potassium hydroxide (AC + KOH)	Particle size (μm)	710–840
	Total surface area (BET, N_2) (m^2/g)	1035
	Average pore diameter (Å)	19.7
Lime (CaO)	Particle size (μm)	590–710
	Total surface area (BET, N_2) (m^2/g)	39
	Average pore diameter (Å)	98.4

[a] AC: activated carbon.
[b] Except the characteristics, other characteristics of activated carbon are obtained from China Activated Carbon Industries Ltd. in Taiwan, ROC.
[c] BET: Brunauer–Emmett–Teller.

2.3. Experimental apparatus and procedure

Fig. 1 shows the pilot-scale incineration system used in this study. The combustor was a bubbling fluidized bed incinerator, consisting of a feedstock feeder and a primary combustion chamber (height = 140 cm, inner diameter (i.d.) = 6.23 cm). A fluidized bed adsorber (height = 45 cm, inner diameter = 8.1 cm) and an impulse fabric filter (air/cloth = 0.28 cm/s), serving as APCDs, were installed after the combustor. The combustion chamber, adsorber and fabric filter were made of stainless steel pipes and sheets. The fluidized bed adsorber was fitted with a distributor made of stainless steel plates with mesh #30, and the bed aspect ratio (bed height/bed diameter = H/D) was about 1.25.

Input air flow rate as calculated by the required amount of theoretical air with an excess air factor of 40% was about 60 l/min at room temperature (25 °C). The operating temperatures of the primary combustion chamber and fluidized bed adsorber were set at 800 and 180–280 °C, respectively. The silica sand added in the combustion chamber and the adsorbent added in fluidized bed adsorber were renewed after each test. When the temperatures reached a steady state, the artificial feedstock was semi-continuously fed into the incinerator at regular intervals of 30 s, and then the impulse fabric filter operation was turned on at the same time. The frequency of the inverse wash of the fabric filter was one time per 90 s. Sampling tasks were started after 5 min and the same sampling time and location of various pollutants were performed on each test. The total operating time of each test was 60 min.

2.4. Sampling and analysis

2.4.1. Acid gases

The acid gases investigated in this study were SO_2 and HCl. The concentration of SO_2 was detected using a flue gas analyzer (BACHARACH model 300). The sampling time periods of each test, prior to and after the fluidized bed adsorber, and after the fabric filter were 15–18, 10–13, and 5–8 min, respectively. The sampling rates were 0.7–1.5 l/min. The analyzer was corrected using the standard gas with determinate concentration before the experiment process. The range of concentration for SO_2 monitoring was 0–1999 ppm, and the accuracy was ± 10 ppm.

The flue gas containing HCl was sampled by a stainless sampling probe and passed through the heated filter holder packed with a glass fiber filter, which collected particles, and the gas then passed through impingers with 100 ml 0.1N sodium hydroxide (NaOH) absorption solution to absorb the HCl gas. The sampling time periods of each test, prior to and after the fluidized bed adsorber, and after the fabric filter were the same (21–31 min). The isokinetic sampling rates were 8 l/min. The analysis of HCl was performed by the method of colorimetry using mercuric thiocyanate (ROC EPA NIEA method A412.70A).

2.4.2. Fine particles

To understand the changes of mass size distribution and elemental size distribution of particles both prior to and after the fluidized bed adsorber, two sets of cascade impactors (Tokyo Dylec Model AS-500) were used to isokinetically sample flue gas prior to and after the fluidized bed adsorber. The sampling time period was 36–39 min and the sampling rates were 8 l/min (Runs 6–10). The size distributions of particles in the range of 0.36–31 μm were determined. The weight difference of each stage of glassy filter before and after sampling was carefully weighed by a microbalance (Mettler-Toledo, AT261) in a clean room where the relative humidity and temperature were controlled at $45 \pm 5\%$ and $25 \pm 1\,^{\circ}C$. After weighing, each stage of glassy filter was pretreated by microwave digestion, and then the concentration of different metals was analyzed by either a furnace atomic absorption spectrometer (FAAS) (Perkin-Elmer A Analyst 100) or a graphite furnace atomic absorption spectrometer (GFAAS) (Perkin-Elmer A Analyst 600).

2.4.3. Heavy metals

The same sampling apparatus and locations used for HCl were also employed to sample metals. For this, the impingers were submerged in an ice bath to enhance condensation, and the mixed absorption divided into two impingers was 100 ml 5% HNO_3 and 100 ml 10% H_2O_2. The sampling time period was 36–41 min and the isokinetic sampling rate was 8 l/min. Just as samples from the impactor, the glassy filter and absorption solution containing metals were pretreated by microwave digestion, and then analyzed by FAAS or GFAAS.

2.4.4. Organics

The organics investigated in this study were gaseous phase polycyclic aromatic hydrocarbons (PAHs) and solid phase PAHs. Isokinetic sampling was also performed. The USEPA modified method 5 (MM5) was used for sampling. The flue gas containing organics was

sampled using a stainless steel sampling probe, which passed the gas through a filter holder housing a glass fiber filter to capture solid phase PAHs, and then passing the gas through a cooling tube to allow the capture of gaseous phase PAHs using XAD-4 resin (6 g). Furthermore, the organic samples were initially extracted for 20 h using a Soxhlet extraction process and the solution was then concentrated to 1 ml using a Kuderno–Danish (KD) evaporative concentrator. Finally, the samples were put into 1.8 ml brown vials and stored at 4 °C, until they were analyzed using a gas chromatograph/flame ionization detector (GC/FID) (Perkin-Elmer Autosystem GC).

3. Results and discussion

3.1. Characteristics of activated carbon

The physical characteristics of activated carbon include BET surface area, average pore diameter and pore volume distribution, both before and after experiments, were analyzed by a micromeritics surface area analyzer (ASAP 2010).

The classification of activated carbon according to pore size could be divided into three parts [12,13], with pore sizes larger than 200 Å defined as "Macropore", between 20 and 200 Å as "Mesopore", and less than 20 Å as "Micropore". Table 4 lists the physical characteristics of activated carbon before and after reaction, indicating that the surface area of activated carbon decreases slightly after immersing with KOH solution and the average pore diameter apparently does not change. The results of the pore volume distribution of AC and AC + KOH before experiment indicate that the total pore volume less than 30 Å

Table 4
Physical characteristics of activated carbon before and after reaction

Run	BET[a] specific surface area (m^2/g)	Reduction of BET specific surface area (m^2/g)	Average pore diameter (Å)
AC[b] (blank)	1075	–	19.7
AC + KOH (blank)	1035	40	19.7
1	935	140	19.8
2[c]	850	185[d]	19.9
3	889	186	20.0
4	835	240	22.1
5	813	262	20.0
6	758	317	19.9
7	738	337	19.8
8	775	300	19.9
9	848	227	19.8
10	556	519	20.2
11	660	415	22.0
12	897	178	19.9

[a] BET: Brunauer–Emmett–Teller.
[b] AC: activated carbon.
[c] Run 2 was the only one test using AC + KOH.
[d] Evaluated as 1035 − 850.

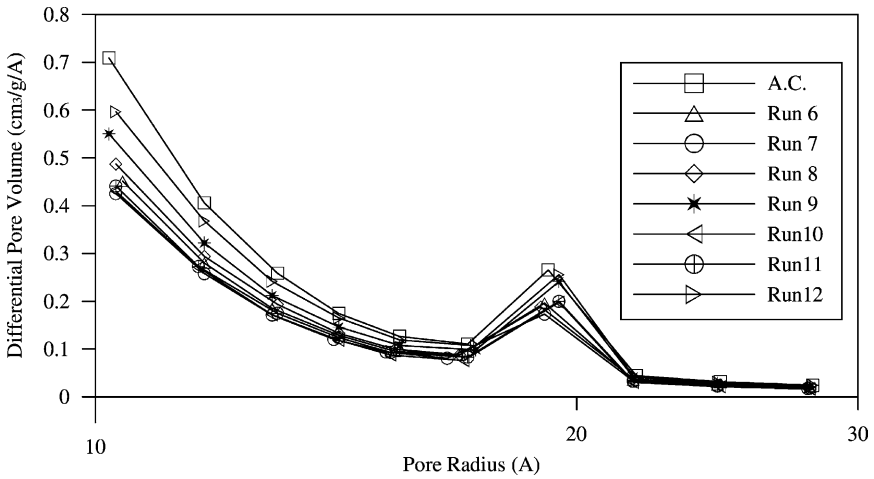

Fig. 2. Pore volume distribution of activated carbon (AC) before and after experiments.

of untreated activated carbon was 2.05 m^3/g, and it decreased to 1.86 m^3/g after immersing with KOH solution. This is because the concentration of KOH (4%) is not high enough to erode the structure of activated carbon, so it does not increase the surface areas as much as expected. On the other hand, the elemental analysis of AC + KOH was also performed. The total percentage of each element, including carbon (C), hydrogen (H), nitrogen (N), oxygen (O) and sulfur (S) was about 80%, and it can be seen that about 20% of potassium ions were present in the activated carbon after immersion in KOH solution. These potassium ions would react with the oxygen functional group on the surface of activated carbon, such as a carboxyl group (–COOH), to form potassium carbonate (K_2CO_3) sedimentation that would block some of the micropores in the activated carbon. Therefore, the surface area of activated carbon decreased slightly after immersion in KOH. Because the amount of saturation adsorption is proportional to the pore volume less than 32 Å [14], the reduction of pore volume of AC + KOH will influence the adsorption of certain pollutants.

Furthermore, because both the surface area and the pore volume of micropores in the activated carbon decreased significantly after experiments (Table 4, Fig. 2), the various pollutants in flue gas not only adsorb or condense on the surface of activated carbon, but also enter the pores by diffusion mechanism, occupying the adsorption sites.

3.2. Control of acid gases

The investigated acid gases in the present study are SO_2 and HCl. Table 5 lists the removal efficiency of SO_2 using a fluidized bed adsorber and the total removal efficiency of SO_2 using a fluidized bed adsorber integrated with a fabric filter. The results indicate that the removal efficiency of the adsorber for SO_2 is 48.8–73.5%, and it reaches over 94% after passing through the fabric filter. Comparing the results of Run 1 with Run 2, the difference in SO_2 removal efficiency of the adsorber is less than 2%. In addition, the reduction surface

Table 5
The concentration and removal efficiency of SO_2

Run	Inlet concentration of fluidized bed adsorber (ppm)	Outlet concentration of fluidized bed adsorber (ppm)	Outlet concentration of fabric filter (ppm)	Removal efficiency of fluidized bed adsorber (%)	Total removal efficiency (%)
1	634.52	281.74	16.967	55.598	97.326
2	606.50	258.21	8.9580	57.426	98.523
3	493.29	149.46	21.004	69.701	95.742
4	519.17	157.31	10.965	69.700	97.888
5	520.31	174.37	4.9898	66.487	99.041
6	393.53	128.61	4.0022	67.319	98.983
7	528.44	154.42	4.9832	70.778	99.057
8	446.89	142.15	7.0162	68.191	98.430
9	395.47	120.13	23.004	69.623	94.183
10	621.14	164.48	5.9878	73.520	99.036
11	422.87	216.69	4.0130	48.757	99.051
12	533.75	198.74	8.0063	62.765	98.500

Note: Removal efficiency of fluidized bed adsorber = [(SO_2 concentration of inlet of fluidized bed adsorber (ppm) − SO_2 concentration of outlet of fluidized bed adsorber (ppm))/SO_2 concentration of inlet of fluidized bed adsorber (ppm)] × 100%. Total removal efficiency = [(SO_2 concentration of inlet of fluidized bed adsorber (ppm) − SO_2 concentration of outlet of fabric filter (ppm))/SO_2 concentration of inlet of fluidized bed adsorber (ppm)] × 100%.

area of AC and AC + KOH are 140 and 185 m^2/g after 60 min (total experiment time), respectively. However, the adsorption amount of SO_2 of AC and AC + KOH are similar during the sampling period. Therefore, the greater reduction of surface area of AC + KOH is not related to the adsorption of SO_2, since it could be caused by adsorption of other pollutants.

Table 6 lists the removal efficiency of HCl by a fluidized bed adsorber and the total removal efficiency of HCl by a fluidized bed adsorber integrated with a fabric filter. The concentration of inlet and outlet of Runs 1 and 2 are close, and it can be stated that the activated carbon did not function at 230 °C, whether or not it was immersed in KOH solution. Nevertheless, with decreasing of flue temperature, the humidity increased and fly ash and elutriation adsorbent filtered on the filter bags could enhance the control of HCl.

Based on these results, the subsequent experiments (Runs 3–5) used untreated activated carbon serving as main adsorbent. Furthermore, different ratios (10–50%) of CaO were added in the adsorber (mixed with activated carbon) in order to enhance the removal of HCl and also raise the removal efficiency of SO_2.

The results of Runs 3–5 reveal that the addition of CaO can raise the removal efficiency of SO_2 by about 14%. However, further increases of CaO (30–50%) does not further increase the efficiency. The addition of CaO causes the reactor to become a binary media reactor, and the change of hydrodynamic behavior could influence the control of SO_2. On the other hand, granular CaO could be abraded to produce finer particles and then be elutriated. Table 6 also reveals the limitation of raising removal efficiency of HCl when CaO is added. Because the addition of more CaO does not function as expected, the following tests used AC + 10% CaO as adsorbent.

Table 6
The concentration and removal efficiency of HCl

Run	Inlet concentration of fluidized bed adsorber (ppm)	Outlet concentration of fluidized bed adsorber (ppm)	Outlet concentration of fabric filter (ppm)	Removal efficiency of fluidized bed adsorber (%)	Total removal efficiency (%)
1	43.52	46.89	2.202	Na[a]	94.94
2	30.55	33.43	2.074	NA	93.21
3	28.46	26.86	1.913	5.62	93.28
4	27.66	28.79	2.135	NA	92.28
5	27.34	24.62	2.072	9.95	92.42
6	20.14	14.85	2.330	26.27	88.43
7	30.23	19.33	2.010	36.06	93.35
8	16.13	16.93	1.976	NA	87.75
9	26.86	23.34	1.945	13.10	92.76
10	38.56	13.89	1.943	63.98	94.96
11	28.79	27.66	1.946	3.92	93.24
12	26.54	23.82	2.168	10.25	91.83

Note: Removal efficiency of fluidized bed adsorber = [(HCl concentration of inlet of fluidized bed adsorber (ppm) − HCl concentration of outlet of fluidized bed adsorber (ppm))/HCl concentration of inlet of fluidized bed adsorber (ppm)] × 100%. Total removal efficiency = [(HCl concentration of inlet of fluidized bed adsorber (ppm) − HCl concentration of outlet of fabric filter (ppm))/HCl concentration of inlet of fluidized bed adsorber (ppm)] × 100%.

[a] NA: not analyzed.

The effects of heavy metals on removal efficiency of SO_2 when the feedstock contains no, single or mixed metals were also investigated (Runs 6–10). The influence of different metals is not significant, but the highest removal efficiency can be obtained when there are no metals in the feedstock (Run 10). The removal efficiency of HCl from Run 10 is also the highest (63.98%). This could be because when the feedstock contains metals, they compete with oxygen and hydrogen ions, reacting with sulfur and chlorine to generate metal sulfate and metal chloride. Therefore, the concentrations of SO_2 and HCl of Run 10 inlet are higher than other tests (Runs 6–9), and higher concentrations of adsorbate generally have higher reaction rates and adsorption amounts. Moreover, the largest decrease of surface area and micropore volume of activated carbon was in Run 10, where the largest amount of pollutants could be adsorbed on the surface of activated carbon. Nonetheless, the removal efficiency of gaseous PAHs was the worst when the feedstock contained no metals. This is because the metals could nucleate or condense on the surface of activated carbon supplying new active sites, and thus enhance the removal of PAHs [15]. Therefore, acid gases and heavy metals could compete for the same adsorption sites on activated carbon.

The effects of adsorption temperature on removal efficiency of acid gases are revealed in the results of Runs 11 and 12. For both SO_2 or HCl, the higher operating temperature (280 °C) provided higher removal efficiency. The adsorption temperature is in direct response to the reaction rate constant, and higher temperatures could increase the reaction rate exponentially, reaching reaction balance more quickly.

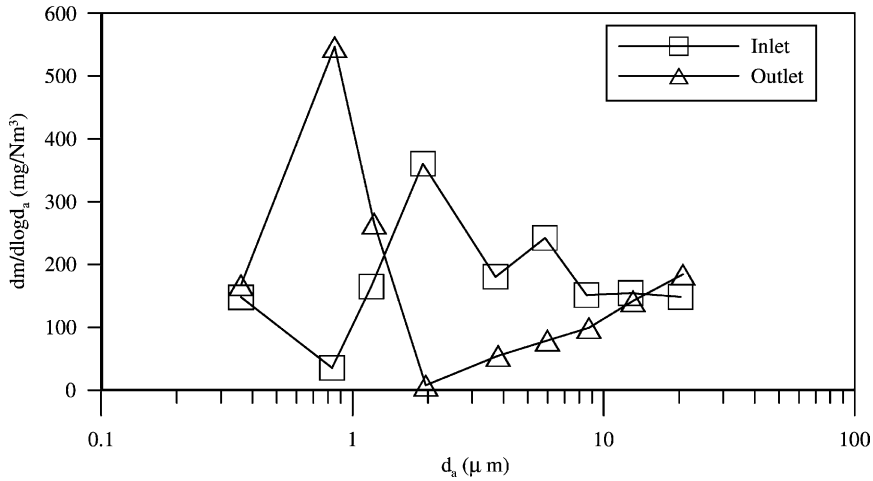

Fig. 3. Mass size distribution of particles at inlet and outlet of fluidized bed adsorber when feedstock contains mixed metals (*Note*: vertical coordinate values = {[weight of certain stage (mg)/(log(maximum particle size of one stage) − log(minimum particle size of one stage))]/sampling volume (N m^3)}; horizontal coordinate values = aerodynamic diameter of particle).

3.3. Mass size distribution of fine particles

The mass size distributions of fine particles prior to and after passing through the fluidized bed adsorber were determined and performed by two sets of cascade impactors. Fig. 3 shows the mass size distribution of the particles at the inlet and the outlet of the fluidized bed adsorber when the feedstock contains mixed metals (Run 9). The integrated area below the curve is the mass concentration of each particle size range. The results indicate that the efficiency for removal particle sizes larger than 1 μm is about 54.2%. However, the mass concentration of particles less than 1 μm of outlet was higher than at the inlet. This may be because particles less than 1 μm are difficult to filter by the fluidized bed adsorber. Due to the abrasion between fluidized medias, the finer particles generated from adsorbent are then collected by the impactor at the outlet. Therefore, the mass concentration of particles less than 1 μm at the outlet is higher than that at the inlet. On the other hand, from the figure of logarithm-probability, the mass–median aerodynamic diameters (MMADs) of inlet and outlet are 2.1 and 1.1 μm, respectively. These results show that the mass size distribution of particles shifted to finer particles size after filtering by adsorber.

3.4. Elemental size distribution of fine particles

The elemental size distribution is defined as the concentration of metals on different particle sizes. From the results of the feedstock containing mixed metals (Pb + Cr + Cd, Run 9), the percentage of each metal at the inlet (sum of all particle sizes) is Pb at 42.95%, Cr at 4.18% and Cd at 52.87%, respectively. The sequence (Cd > Pb > Cr) is consistent with the volatility of metals. Liu et al. [16] also showed that the proportion of five metals

Table 7
Total concentration (Pb + Cd + Cr) and removal efficiency of metals

Run	Inlet concentration of fluidized bed adsorber (mg/(N m^3))	Outlet concentration of fluidized bed adsorber (mg/(N m^3))	Outlet concentration of fabric filter (mg/(N m^3))	Removal efficiency of fluidized bed adsorber (%)	Total removal efficiency (%)
1	311.15	219.00	0.3920	29.62	99.874
2	317.48	182.25	0.3746	42.595	99.882
3	394.45	200.78	0.3156	49.099	99.920
4	310.78	231.58	0.3170	25.48	99.898
5	343.90	174.90	0.2889	49.142	99.916
11	325.70	163.30	0.3355	49.862	99.897
12	349.85	182.70	0.3359	47.778	99.904

(Cd, Zn, Pb, Cr and Cu) follows the order Cd > Zn > Pb > Cr > Cu, in accordance with the volatility of those metals. The tendency of the distribution at the adsorber outlet is similar to that at the inlet.

3.5. Control of metals

Table 7 lists the total concentration of metals (Pb + Cd + Cr) at the inlet and outlet of fluidized bed adsorber, and the removal efficiency of metals. The results indicate that the adsorber has 25–50% removal ability, increasing to almost 100% after passing through a fabric filter. The activated carbon immersed in KOH (RE = 42.6%) is more effective than untreated activated carbon (RE = 29.6%). The adsorption amount of AC + KOH after experiment (60 min) is 0.15 (mg metals/g AC + KOH) higher than AC, which shows once again that AC + KOH is more effective in controlling metals. On the other hand, although CaO can capture heavy metals, the changes in the hydrodynamic behavior of the adsorber also reduce the adsorption amount of AC. Thereby, the removal efficiency of metals also decreases after adding CaO (Runs 3–5). Finally, with higher adsorption temperatures, there were greater adsorption amounts of metal obtained (Run 12 (7.11 mg/g) > Run 3 (5.06 mg/g) > Run 11 (3.42 mg/g)). It can be concluded that the main mechanism of removal of metals on activated carbon is chemisorption.

3.6. Control of PAHs

Comparing AC with AC + KOH, the removal efficiency of gaseous phase PAHs of untreated activated carbon is more effective than AC+KOH. Because the amount of surface oxygen functional group increases after immersing in KOH solution, the elemental structure of activated carbon tends to be more polar, which makes it difficult for the PAHs with no polarity or weak polarity to be adsorbed. Regarding adsorption temperature, when using a temperature (280 °C) that is higher than the boiling points of some PAH species, the PAH species may volatilize or desorb after being adsorbed on activated carbon. Therefore, high temperature is unfavorable to control gaseous phase PAHs.

Because the solid phase PAHs are defined as PAHs on particles of glass fiber filter, the removal efficiency of solid phase PAHs of a fluidized bed adsorber depends on the removal ability of particles. The removal efficiencies of all tests were 92–97%. Moreover, the relationship between particle size and concentration of PAHs is insignificant [17] and the average concentration of PAHs sampled on fly ash prior to and after passing through the adsorber of each test is similar. Therefore, the removal efficiency of solid phase PAHs does not significantly differ under various operating conditions.

4. Conclusions

A fluidized bed adsorber integrated with a fabric filter was employed to control acid gases produced from incineration. The removal efficiencies of the investigated acid gases, SO_2 and HCl, were higher than 94 and 87%. Along with removal of sulfur and HCl, the combination of a fluidized bed adsorber and a fabric filter can also control organics and heavy metals at the same time. Furthermore, although particles less than 1 μm are difficult to filter using a fluidized bed reactor, particles larger than 1 μm (less than 31 μm) could partially be removed (removal efficiency = 54.2%). Previous studies also showed that particles larger than 34.1 μm could generally be filtered using a fluidized bed adsorber [10]. Furthermore, based on economic and engineering viewpoints, activated carbon also has advantages over other adsorbents. Thus, a fluidized bed adsorber integrated with a fabric filter can replace conventional APCDs such as a semi-dry (or dry) system integrated with a fabric filter or electrostatic precipitator integrated with a wet scrubber. The pilot-scale experiment performed in this study permits detection of features and phenomena which cannot be detected in small scale experimental set-ups, which use simulated feed streams which are usually not very realistic. However, the detailed reaction between various pollutants or scale up of the fluidized bed adsorber requires further study.

References

[1] I. Mochida, Y. Korai, M. Shirahama, S. Kawano, T. Hada, Y. Seo, M. Yoshikawa, A. Yasutake, Removal of SO_x and NO_x over activated carbon fibers, Carbon 38 (2000) 227–239.
[2] A.A. Lizzio, J.A. DeBarr, Effect of surface area and chemisorbed oxygen on the SO_2 adsorption capacity of activated char, Fuel 75 (1996) 1515–1522.
[3] B. Rubio, M.T. Izquierdo, Influence of low-rank coal char properties on their SO_2 removal capacity from flue gases. I. Non-activated chars, Carbon 35 (1997) 1005–1011.
[4] A. Lisovskii, R. Semiat, C. Aharoni, Adsorption of sulfur dioxide by active carbon treated by nitric acid. I. Effect of the treatment on adsorption of SO_2 and extractability of the acid formed, Carbon 35 (1997) 1639–1643.
[5] B. Rubio, M.T. Izquierdo, A.M. Mastral, Influence of low-rank coal char properties on their SO_2 removal capacity from flue gases. 2. Activated chars, Carbon 36 (1998) 263–268.
[6] P. Davini, Desulphurization properties of active carbons obtained from petroleum pitch pyrolysis, Carbon 37 (1999) 1363–1371.
[7] A.A. Lizzio, J.A. DeBarr, Mechanism of SO_2 removal by carbon, Energy Fuels 11 (1997) 284–291.
[8] P. Davini, The effect of certain metallic derivatives on the adsorption of sulphur dioxide on active carbon, Carbon 39 (2001) 419–424.

[9] E. Raymundo-Piñero, D. Cazorla-Amorós, C. Salinas-Martinez de Lecea, A. Linares-Solano, Factors controlling the SO_2 removal by porous carbons: relevance of the SO_2 oxidation step, Carbon 38 (2000) 335–344.
[10] B.C. Chiang, M.Y. Wey, W.Y. Yang, Control of incinerator organics by fluidized bed activated carbon adsorber, J. Environ. Eng. ASCE 126 (2000) 985–992.
[11] D. Geldart, M. Rhodes, Developments in fluidization, Chem. Eng. 2 (1986) 30–32.
[12] M.M. Dubinin, Adsorption properties and microporous structures of carbonaceous adsorbents, Carbon 25 (1987) 593–598.
[13] M.M. Dubinin, N.S. Polyakov, L.I. Kataeva, Basic properties of equations for physical vapor adsorption in micropores of carbon adsorbents assuming a normal micropore distribution, Carbon 29 (1991) 481–488.
[14] K. Urano, S. Ornori, E. Yamamoto, Prediction method for adsorption capacities of commercial activated carbons in removal of organic vapors, Environ. Sci. Technol. 16 (1982) 10–14.
[15] M.Y. Wey, L.J. Yu, S.I. Jou, The influence of heavy metals on the formation of organics and HCl during incinerating of PVC-containing waste, J. Hazard. Mater. 60 (1998) 259–270.
[16] Z.S. Liu, M.Y. Wey, C.L. Lin, The capture of heavy metals from incineration using a spray–dryer integrated with a fabric filter using various additives, J. Air Waste Manage. Assoc. 51 (2001) 983–991.
[17] M.Y. Wey, C.Y. Chao, J.C. Chen, L.J. Yu, The relationship between the quantity of heavy metal and PAHs in fly ash, J. Air Waste Manage. Assoc. 48 (1998) 750–756.